Reviews in Mineralogy & Geochemistry
Vol. 84 pp. XXX-XXX, 2018
Copyright © Mineralogical Society of America

High Temperature Reactions Between ~~Gas~~ and Ash Particles in Volcanic Eruption Plumes

Pierre Delmelle
Earth and Life Institute—Environmental Sciences
Université catholique de Louvain
B-1348 Louvain-la-Neuve
Belgium
pierre.delmelle@uclouvain.be

Fabian B. Wadsworth
Department of Earth and Environmental Sciences
Ludwig-Maximilians University Munich
80333 Munich
Germany
fabian.wadsworth@min.uni-muenchen.de

Elena C. Maters
Institute for Climate and Atmospheric Science
School of Earth and Environment
University of Leeds
LS6 9JT Leeds
United Kingdom
e.c.maters@leeds.ac.uk

Paul M. Ayris
Department of Earth and Environmental Sciences
Ludwig-Maximilians University Munich
80333 Munich
Germany
pmayris@gmail.com

INTRODUCTION

The common manifestation of an explosive volcanic eruption is the emission of a hot mixture of solid fragments and expanding magmatic gases, referred to as the eruption plume, into the atmosphere (Fig. 1, Sparks et al. 1997; Carey and Bursik 2015). Ash (the rock particles less than two millimeters across) usually dominates the plume's solid load, whereas water vapor followed by CO_2 and lesser amounts of sulfur and halogen species constitute the eruptive gas phase. Plumes can initially travel at jet with velocities up to 600 ms^{-1}, temperatures above 800 °C and densities of a few kgm^{-3}, reaching five to ten times the density of the ambient air. However, rapid cooling and dilution of the ash and gas occurs when the plume entrains and heats the surrounding air, generating buoyancy and uplift. Thus, eruption plumes are characterized by strong temperature, chemical and density gradients, offering ample opportunities for heterogeneous reactions between volcanic gases and ash particles.

1529-6466/18/0084-0006$05.00 (print)
1943-6266/18/0084-0006$05.00 (online)
http://dx.doi.org/10.2138/rmg.2018.84.8



Figure 1. An eruption plume generated by the explosive eruption of Soufrière Hills volcano, Montserrat, on 11 February 2010 following a partial dome collapse. The eruption lasted for less than two hours with the plume reaching an altitude of ~15 km above sea level. Image courtesy of Bernard Royer.

It has long been recognized that in-plume gas–ash interactions play a role in scavenging magmatic volatiles (e.g., sulfur and halogens) and emplacing soluble compounds on ash surfaces (Witham et al. 2005; Ayris and Delmelle 2012, and references therein). Indirect evidence comes from ash leachate studies which attribute the rapid mobilization of an array of cations and anions upon exposure of ash to water to the presence of mixed sulfate and halide salt deposits (Taylor and Stoiber 1973; Rose 1977; Óskarsson 1980). Some studies have argued that in-plume gas–ash interactions may remove up to ~30–40% of sulfur and ~10–30% of chlorine emitted by explosive eruptions (e.g., Rose 1977; Varekamp et al. 1984; de Hoog et al. 2001; de Moor et al. 2005). This potentially contributes to a reduction of the impacts of volcanic plumes on atmospheric chemistry and climate (Tie and Brasseur 1995; Robock 2000; Grainger and Highwood 2003; von Glasow et al. 2009). On the other hand, the release of sulfate and halide compounds from ash surfaces may have various effects in terrestrial or aquatic environments receiving ash fall (Ayris and Delmelle 2012, and references therein). An established concern for agricultural and health authorities, such as after the 2010 Eyjafjallajoküll eruption in Iceland, is linked to the burden of potentially toxic soluble elements including fluorine in ash (Thorarinsson 1979; Cronin et al. 2003; Dawson et al. 2011; Gislason et al. 2011). Conversely, ash deposits impact positively on soil fertility by rejuvenating the mineral reservoir of macronutrients such as calcium, potassium and magnesium (Dahlgren et al. 2004). Similarly, ash fallout may have a beneficial influence on primary productivity in iron-limited regions by providing iron, a micronutrient essential to phytoplankton growth (Duggen et al. 2010, and references therein; Hamme et al. 2010).

Reactions occuring during ash transit through distinct temperature zones in the eruption plume (Fig. 2) are held responsible for magmatic volatile scavenging leading to the various and poorly described sulfate and halide salts on ash surfaces (Rose 1977; Óskarsson 1980). Some have posited that such salts form by homogeneous nucleation and growth at magmatic temperatures (600–1200 °C) and then deposit as sublimates onto ash particles (Taylor and

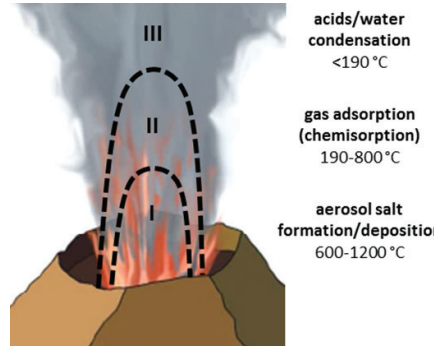


Figure 2. Schematic of the three temperature-dependent reaction zones in an explosive eruption plume. Salts may (I) be deposited directly onto ash as sulfate and halide salt aerosols formed at magmatic temperatures (600–1200 °C), (II) form by reaction with gaseous SO_2, HCl or HF adsorbed (chemisorbed) onto ash at magmatic down to sulfuric acid dewpoint temperatures (~190–200 °C), and/or (III) be a product (precipitate) of partial leaching and dissolution of ash in contact with sulfuric and halogen acid condensates at temperatures < 190 °C.

Stoiber 1973; Smith et al. 1983). Others have emphasized the conceptual (but still unverified) model that at low temperatures (below the sulfuric acid dewpoint ~190–200 °C) ash particles act as condensation nuclei for sulfuric/hydrochloric/hydrofluoric acids and liquid water (Rose 1977; Hinkley and Smith 1982; Delmelle et al. 2007). The resulting acidic aqueous solution can react with the ash surface and dissolve its glass and mineral constituents, eventually leading to the precipitation of sulfate and halide salts.

Until recently, in-plume reactions at higher temperatures (above ~190–200 °C) between the eruptive gas phase and ash particles have received little attention, as they have been regarded as comparatively inefficient (Rose 1977). In addition, such interactions within the dangerous and complex environment of a volcanic eruption plume are opaque to direct analysis. However, high temperature heterogeneous reactions, if effective, may remove significant amounts of magmatic sulfur, chlorine and fluorine from the gas–ash mixture immediately after magma fragmentation. Consequently, these reactions may modify ash surface properties (e.g., hygroscopicity, acidity/basicity, redox speciation) early in a plume's evolution, with important ramifications for later chemical and physical processes at lower temperatures in the subaerial environment (e.g., ash particle aggregation, trace gas uptake on ash, iron release from ash; Maters et al. 2016, 2017a,b; Mueller et al. 2017). Therefore, a better appraisal of heterogeneous gas–ash reactions not only may impact our understanding of various volcanic processes, but also has wider environmental and societal significance.

Ash leachate studies may identify and quantify the soluble elements adsorbed on ash during gas–ash interactions within the eruption plume, including sulfur, chlorine and fluorine. However, these studies provide only limited mechanistic insights into the reactions and the factors that control them. Recently, a new era of experiment-based investigations, in which the temperature and chemical conditions found within the hot plume core are simulated, has emerged. These have led to notable progress in our understanding of high temperature uptake and reactions of volcanic gases, specifically SO_2 and HCl on ash. In this chapter, we briefly describe the generation and composition of eruption plumes as relevant to high temperature gas–ash interactions, give an overview of recent experimental approaches used to study such interactions, review the findings of laboratory studies on the uptake and reactions of SO_2 and HCl gases on aluminosilicate glass materials, and discuss the implications of these findings in terms of sulfur and chlorine scavenging by ash in explosive eruption plumes.

ERUPTION PLUME: GENERATION, COMPOSITION AND TEMPERATURE

From a physical point of view, eruption plumes are composed of a gas phase and a solid load. From a chemical point of view, both the gas and the solid components may vary from volcano to volcano, and even from eruption to eruption, and change with time. From a thermal point of view, plumes cool as they expand and mix with ambient air. Here we review the formation of a plume and the evolution of its composition and temperature.

Generation

Volcanic eruption plumes are primarily the result of magma fragmentation, i.e., the sub-surface process that transforms a silicate magma with dispersed gas bubbles into solid fragments (pyroclasts) dispersed in a gas phase (Cashman and Scheu 2015). Magma fragmentation is driven by the exsolution from the melt of a few weight percent of volatiles, mostly water followed by CO_2 and lesser amounts of sulfur and halogens (Sparks et al. 1997; Cashman and Scheu 2015). Exsolution of volatiles and their subsequent concentration in gas bubbles start when the volatile solubility is exceeded in the magma, typically in response to a drop in lithostatic pressure (Burgisser and Degruyter 2015).

Diffusive transfer of water from the melt to the gas bubbles dehydrates the melt and can cause crystal phases to grow, both of which result in a bulk increase in magma viscosity (Hess and Dingwell 1996; Mader et al. 2013). If the newly formed gas phase cannot escape freely through permeable networks, bubbles grow within the rising magma by both continued volatile exsolution and gas expansion in response to decreasing pressure. This lowers the density and increases the volume of the magma, which in turn accelerates its ascent towards the surface while triggering more bubble growth by volatile exsolution and expansion. This cascade of events leads to high strain rates at expanding bubble walls in the hot magma foam, eventually causing it to fragment within the volcanic conduit or surficial dome (Cashman and Scheu 2015).

In explosive eruptions, this fragmentation transition occurs due to locally unrelaxed liquid behavior at the walls of expanding bubbles (Kameda et al. 2013) and the resultant pervasive propagation of fractures between bubbles. The magnitude of the pressure-drop that drives both bubble expansion below the fragmentation level, and the acceleration of the ash particles above, is a controlling factor in the particle size distribution produced (Kueppers et al. 2006; Fowler and Scheu 2016). In turn, this particle size distribution—and in detail, the specific surface area—is a controlling factor in the efficiency of high temperature gas–ash reactions above fragmentation.

Composition

At the point of exit, an eruption plume is made up of ~1–10 wt% of gas and ~90–99 wt% of ash (Sparks et al. 1997), but the precise componentry is not known. A scarcity of plume gas composition data in this proximal in- or near-vent region relates in large part to the danger and difficulty of acquiring accurate measurements within a dense and opaque eruptive plume. Instead, high temperature volcanic gas compositions have been measured in fumaroles or in near-vent plumes of degassing volcanoes by various techniques including direct sampling and remote sensing. These compositions can be highly variable, with measurements across eight different volcanoes ranging from 79–97 mol% H_2O, 0.5 to 12 mol% CO_2, 0.2–6.5 mol% SO_2, 0.1–0.6 mol% H_2S, <0.1–1.5 mol% H_2, 0.2–0.8 mol% HCl, <0.1 mol% HF and <0.1–0.5 mol% CO (Fischer and Chiodini 2015, and references therein). Measurements from various divergent plate (rift), intraplate (hot spot), and convergent plate (arc) volcanic settings show compositions with comparatively high proportions of CO_2 (up to 13 mol%), SO_2 (up to 19 mol%), and HCl (up to 2 mol%), respectively (Gerlach 2004).

Numerical models may be used to predict plume gas compositions. By simulating mixing of a given set of CO_2-, SO_2- and HCl-rich volcanic gas compositions at 1000 °C with ambient air using a one-dimensional numerical model, Hoshyaripour et al. (2015) calculated the following ranges of plume gas compositions at 600 °C: 50–58 mol% H_2O, 2–9 mol% CO_2, 0.4–4 mol% SO_2, 0.9–3 mol% SO_3, <0.1 mol% H_2SO_4, <0.1 mol% H_2S, <0.1 mol% H_2, 0.1–0.5 mol% HCl, <0.1–0.3 mol% HF, 0.1–0.2 mol% CO, 2.5–5 mol% O_2 and 32–34 mol% N_2. Air entrainment leads not only to dilution of the volcanic gases but also to a change in the redox conditions of the plume gas phase, with increasing proportions of oxidized species such as SO_2, SO_3 and H_2SO_4 relative to reduced sulfur species, i.e., H_2S, upon exposure to oxygen at high temperatures (Hoshyaripour et al. 2012).

Ash coexists with magmatic gases in eruption plumes. The ash has a bulk chemical composition ranging from basaltic to rhyolitic, with an increase in SiO_2 content typically accompanied by a decrease in FeO/Fe_2O_3, MgO and CaO contents (<10 wt% each; Fisher and Schmincke 1984). Ash mineralogy is dictated by its source magma and is comprised of a mixture of aluminosilicate glass; an amorphous material quenched from the melt, and crystalline minerals originating from the crystals formed during magma ascent (Heiken and Wohletz 1992).

The structure of aluminosilicate glass depends on its chemical composition and consists of a random three-dimensional network of tetrahedral units (Scholze 1990; Mysen and Richet 2005). These tetrahedra are made up of network formers; elements with coordination numbers of 3 or 4 including Si^{4+}, Al^{3+} and in some cases Fe^{3+}, and bridging oxygen atoms (BO) that are shared between two network formers. Network modifiers; elements such as ~~Na, Ca and Mg~~, depolymerize the silicate network and are bonded to tetrahedra by non-bridging oxygens (NBO; oxygen atoms that are bonded to only one network former). These cations usually have a coordination number of 6. In the presence of trivalent cations in tetrahedra (network formers), such as Al^{3+} and Fe^{3+}, alkali and alkaline earth cations will occur in close proximity to the tetrahedra to provide an overall neutral charge. These cations are referred to as charge compensators and contribute to increasing the connectivity of the network.

Ash crystallinity typically ranges from 0–60 vol% depending on factors such as the composition, temperature and supply (and hence ascent) rate of the magma (Heiken and Wohletz 1992). Minerals that occur in basaltic ash include olivine, pyroxene, Ca-rich plagioclase, and Fe-Ti oxides, while those most common in rhyolitic ash include quartz, hornblende, biotite, Na-rich plagioclase and alkali feldspars. Minerals in ash have been found to be overlain by a thin glass coating, suggesting that ash surfaces may be predominantly glassy, although crystalline phases may be exposed by fracture/abrasion of the ash (Heiken and Wohletz 1992; Jones et al. 2016).

Two physical properties that impact the reactivity of a solid substrate towards gaseous species are microporosity and specific surface area. Ash is essentially a non-porous material devoid of micropores (<2 nm in diameter) and otherwise dominated by macropores (>50 nm in diameter; Delmelle et al. 2005). The specific surface area of ash is inversely related to particle size and typically ranges from ~0.5–2 $m^2\ g^{-1}$ as normally measured by nitrogen or krypton gas adsorption techniques. Variations in mineralogy, shape and surface texture/morphology (illustrated in Fig. 3) are responsible for the higher specific surface areas actually measured for natural powders such as ash relative to those calculated based on an approximation of spherical (or other simple geometrically shaped) particles (Brantley 2003; Riley et al. 2003). The ratio of specific surface area measured by gas adsorption to the geometric surface area defines the surface roughness (Helgeson et al. 1984).

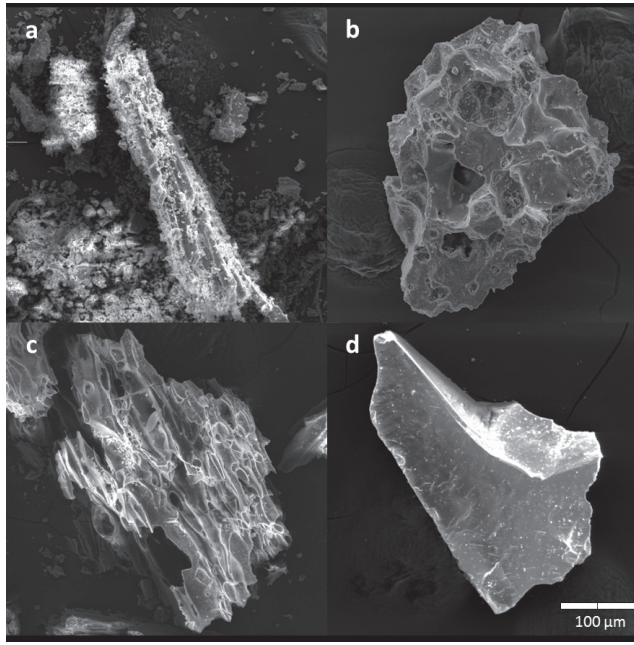


Figure 3. Scanning electron microscopy images of ash particles from the eruptions of (a) Pinatubo volcano, Philippines, in 1991, (b) Eyjafjallajökull volcano, Iceland, in 2010, and (c and d) Chaitén volcano, Chile, in 2008. Images acquired at 15 kV using a Tescan VEGA II instrument.

Temperature

Insight into the complex dynamics of temperature within eruption plumes is largely provided by numerical models. A three-dimensional numerical model combining pseudo-gas and Lagrangian models for fluid and particle motion, respectively, has been applied to simulate ejection of a volcanic gas and solid pyroclast mixture from a circular vent above a flat surface into a stratified atmosphere (Suzuki et al. 2005; Suzuki and Koyaguchi 2012). The velocity and temperature of the gas and solid phases (including ash) are deemed equivalent based on an assumption of very rapid exchanges of momentum and heat between them. At eruptive temperatures (800–1200 °C) or lower, cooling mechanisms of ash in eruption plumes are dominated by conductive transfer of heat to the surface of the ash particle and both conductive and convective transfer into the plume gas (Wadsworth et al. 2017). This occurs rapidly because ash particles are small and thermal diffusivities in volcanic ash are generally high (~10^{-7} $m^2 s^{-1}$ for dense rhyolitic glassy ash; Bagdassarov and Dingwell 1994).

To predict the thermal regime experienced by ash in an explosive eruption plume, Ayris et al. (2014) considered two contrasting eruption scenarios (volcanic explosivity indices of 3–4 and >5) with magma discharge rates of 10^6 and 10^9 $kg s^{-1}$ and erupted magma volumes of 0.01–0.1 and >1 km^3. The three-dimensional model described above predicts that fine ash particles (<63 µm in diameter) are sustained at near-magmatic temperatures for 13 and 60 s on average, respectively, based on these scenarios. Subsequent cooling at rates of −50 and −5 °C s^{-1} on average takes place over 7 and 110 s, respectively, down to the sulfuric acid (H_2SO_4) dewpoint temperature (~190–200 °C). Therefore, in addition to the potential for mixing of gases and pyroclasts in the sub-surface volcanic conduit (also lasting several to tens of seconds; Ayris et al. 2013), the time interval available for high temperature gas–ash interaction may be on the scale of minutes in Earth's largest explosive eruptions.

METHOD OF INVESTIGATING THE HIGH TEMPERATURE REACTIONS OF VOLCANIC GASES ON ASH

Aluminosilicate glass as a proxy for volcanic ash

The pre-existing and unknown reaction history of natural ash particles collected near and/or far from volcanic vents creates some uncertainity in using them as starting material for simulating high temperature gas–ash interaction in the laboratory. Therefore, recent studies have used natural or synthetic aluminosilicate glass as a proxy for ash as it normally represents the dominant component of ash (Ayris et al. 2013, 2014; Palm et al. 2018, this volume; Renggli and King 2018, this volume). While the presence of significant crystalline components in natural ash may limit aluminosilicate glass as a fully representative analogue, in general ash particle outer layers—which provide the interface for heterogeneous gas–ash interaction—are typically glassy, even if the glass is coating sub-surface mineral constituents (Heiken and Wohletz 1992).

Suitable aluminosilicate glass compositions can be obtained by melting and sintering fresh volcanic rock fragments above the liquidus and quenching the homogenized silicate melts at atmospheric pressure. Alternatively, simplified aluminosilicate glass compositions can be synthesized by melting and quenching mixtures of pure oxides, hydroxides and/or carbonates (e.g., SiO_2, Fe_2O_3, $Al(OH)_3$, $MgCO_3$, $Mg(OH)_2$, $CaCO_3$, etc.) in known proportions (e.g., Holloway and Wood 1988; Palm et al. 2018, this volume). Prior to experiments of gas uptake, the glass material is crushed to powder (particle size < 100 µm in diameter) under dry conditions or in acetone. Glass wafers may also be used instead of powders as the former material is better suited for surface-sensitive analyses (e.g., Palm et al. 2018, this volume).

The quenching of synthetic glasses imparts a thermal history during glass formation that may be somewhat different from the thermal history experienced by volcanic ash during its formation, i.e., the synthetic ash surfaces may relax over a different window of temperatures during experimentation compared to that in which natural ash would relax (Gottsmann et al. 2002). This should be kept in mind when interpreting the results of experiments performed in the glass transition temperature interval, as the glass structure may affect the rates of reaction with gases at high temperatures (Renggli and King 2018, this volume).

Experimental apparatus

In order to gain insight into the high temperature uptake and reaction of SO_2 and HCl gases on ash, Ayris et al. (2013, 2014) used a quartz reactor tube placed within a temperature-controlled tube furnace held vertically or horizontally. Briefly, approximately 1 g of powdered aluminosilicate glass was packed in the quartz tube and heated to the desired experimental temperature under a helium gas stream prior to flushing with a SO_2 or HCl gas flow for a given period of time. While easy to use, this apparatus had limited capabilities for simulating the complex composition of an eruptive gas phase and for varying the gas:solid ratio.

Recently, a unique reactor has been developed for studying gas–ash interaction in eruption plumes (Fig. 4). The novel instrument—the so-called Advanced Gas–Ash Reactor—operates at temperatures ranging from 200 to 900 °C, is capable of generating a gas mixture comprised of H_2O, CO_2, SO_2 and HCl, and can hold < 1–10 g of ash. Only a brief explanation of the instrument design and operational conditions is given here; a full description is available in Ayris et al. (2015). The Advanced Gas–ash Reactor features a horizontal furnace that hosts a rotating quartz tube in which a separate sample bulb can be inserted. A gas-injector assembly connected to gas mass-flow controllers and a nebulizer for aerosolizing deionized water allows the generation of an array of gas and water flow rates.

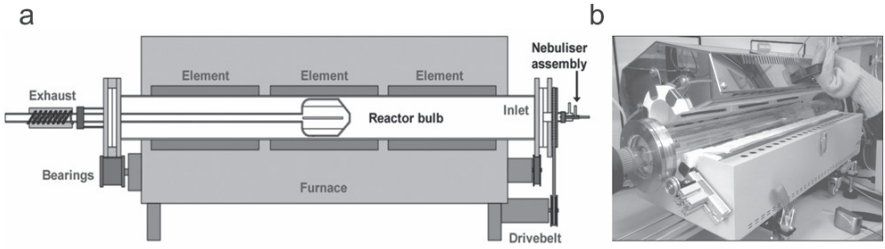


Figure 4. (a) Schematic and (b) photo of the Advanced Gas–Ash Reactor showing key parts including the three-stage furnace and its heating elements, the quartz tube with the inserted rod and sample (reactor) bulb, and the gas inlet and outlet (exhaust).

The device is able to produce mixtures of gas compositions within the range of those measured near volcanic vents. It can also accommodate a large variety of heating and cooling rates (heating to eruptive temperatures at up to +20 °C s^{-1} or cooling from eruptive temperatures at up to −10 °C s^{-1}), but it does not simulate all pressure regimes and fluid dynamic conditions found within a volcanic conduit or eruption plume. For further discussion of experimental set-ups for gas-solid reactions within a more general context, readers are referred to King et al. (2018, this volume).

Post-experiment analysis

Characterization of the glass powders before and after experimental treatment is necessary to elucidate the products and/or potential mechanisms of aluminosilicate glass reaction with various gases. The particle size distribution and specific surface area of the glass materials are measured by laser diffraction and nitrogen or krypton gas adsorption, respectively. The glass bulk and surface chemical compositions are measured by X-ray fluorescence and X-ray photoelectron spectroscopy (XPS), respectively, while the presence and identity of any crystalline minerals in abundances >5wt% is assessed by X-ray diffraction (XRD). The amount of readily soluble compounds on glass surfaces is determined by leaching of the samples in ultrapure water, followed by analysis of the filtered leachates for dissolved element concentrations by ion chromatography (SO_4^{2-}, Cl^-) and atomic absorption/emission spectroscopy or mass spectrometry (Al, Fe, Mg, Ca, Na, K). The dissolved SO_4^{2-} and Cl^- concentrations are used as a measure of, respectively, SO_2 and HCl gas uptake on the glass materials. Raman spectroscopy, Fourier transform infrared spectroscopy (Mernagh et al. 2018, this volume), and scanning and transmission electron microscopy coupled with energy dispersive X-ray spectroscopy (SEM- and TEM-EDX) can be used to examine regions of the glass surfaces, for instance to detect enrichments/depletions in certain elements or the occurrence of specific compounds, including salt deposits (e.g., $CaSO_4$, NaCl). Higher resolution techniques applied to analyse and/or image reaction products at the nanometer scale include atom probe microscopy, grazing incident angle XRD, nano secondary ion mass spectrometry (nano-SIMS), and depth profiling using XPS or SIMS (Dalby et al. 2018, this volume; Palm et al. 2018, this volume).

HIGH TEMPERATURE UPTAKE AND REACTION OF SULFUR DIOXIDE AND HYDROGEN CHLORIDE GASES WITH ALUMINOSILICATE GLASS

The necessary first step in any heterogeneous gas-solid reaction involves activation of the gas molecule by chemisorption onto the solid surface. Chemisorption entails formation of a chemical bond between the molecule and the surface; it is accompanied by a significant enthalpy change, typically greater than 80 kJmol^{-1} (Atkins and Jones 1999). In order for a chemical bond to form, chemisorption must take place at a specific reactive site on the solid surface.

Therefore, once all available reactive surface sites are occupied, no additional molecules can be chemisorbed. This implies that only a single layer (a monolayer) of chemisorbed molecules is possible. Although any gas molecule may also weakly interact with the solid surface through van der Waals forces (the enthalpy change is typically 40 kJ mol^{-1} or less), it is not thereby activated for heterogeneous reaction. Nevertheless, physisorbed molecules may serve as precursors to chemisorbed molecules. The physical location at which adsorption of a molecule takes place on a surface is referred to as an 'adsorption site.'

Aluminosilicate glasses are amorphous and contain various elements in different coordinations, giving rise to an array of adsorption sites which are not chemically, structurally, or topologically ordered. A rationale similar to that developed to explain the strength of acidic and basic sites exposed on silica glass and metal oxide surfaces may be used to describe the nature of surface adsorption sites on an aluminosilicate glass. The surface sites on these materials are comprised of hydroxyl (≡Si–OH and ≡M–OH), siloxane (≡Si–O–Si≡) and oxo (≡Si–O and ≡M–O) groups as well as coordinatively unsaturated terminal metal (≡M) atoms with slight positive charge (e.g., Carre et al. 1992; Legrand 1998). At high temperatures, the surface hydroxyl groups become unstable and may break down; for example silanols (≡Si–OH) condense to form siloxane bridges (McDonald 1958). The remaining ≡Si–O-bearing groups behave as Lewis acids (electron-accepting) with slightly positive charge available to react with gas species. Terminal M atoms in complex aluminosilicates have a vacant electronic orbital and also behave as Lewis acids. The acid and base strength of the remaining metal oxo groups depends on the ionic character percentage of the ≡M–O bond and the charge-to-radius ratio of the metal (e.g., Fripiat et al. 1965; Tanabe et al. 1989; Auroux and Gervasini 1990). Thus, SiO_2 has surface acidic sites, amphoteric oxides such as Al_2O_3 contain both acidic and basic sites, whereas alkali and alkaline earth oxides display distinct surface basic (electron-donating) characteristics (Paukshtis et al. 1979; Auroux and Gervasini 1990).

In aluminosilicate glass, both the network former (Si^{4+}, Al^{3+}, Fe^{3+}) and network modifier (Na^+, K^+, Ca^{2+}, Mg^{2+}, Fe^{2+}) cations are covalently linked to O, engendering surface sites of the oxo group type. Maters et al. (2016) showed that the surface of volcanic glass is multifunctional, combining acidic, basic, oxidizing and reducing sites in various proportions, a characteristic expected for a complex amorphous solid. These authors also inferred that the density of total basic surface sites correlates positively with the total Na, K, Ca and Mg content of the glass surface. As discussed below and by Renggli and King (2018, this volume), other factors such as glass structure and proximity to the glass transition temperature may also play a role in gas-glass reaction mechanisms and rates. Overall, the structural and chemical heterogeneity of aluminosilicate glass surfaces makes interfacial chemical reaction mechanisms of these surfaces particularly challenging to study and model theoretically.

Sulfur dioxide uptake and reaction

Sulfur dioxide gas released from erupting magmas and injected into the stratosphere is converted to sulfate aerosols, which contribute to climate cooling by reflecting incoming solar radiation. An improved understanding of the fate of SO_2 gas in eruption plumes is important for constraining volcanic sulfur budgets, and hence assessing potential volcanic forcing of climate. It has traditionally been assumed that in-plume SO_2 scavenging, estimated to reduce stratospheric SO_2 injection by up to 40%, is driven by interaction with water, ice and/or ash below the acid dewpoint temperature (i.e., involving liquid H_2SO_4; Rose 1977; Textor et al. 2003). A role of high temperature gas–ash interaction as a sink for volcanic SO_2 has largely been overlooked. However, in light of previous studies showing that gaseous SO_2 reacts with soda-lime–silica glass compositions at high temperatures (e.g., Douglas and Isard 1949), the abundance of sulfate salts (mainly calcium sulfate, $CaSO_4$) on volcanic ash may evidence significant uptake of SO_2 in the hot eruption plume.

Ayris et al. (2013) investigated the influence of temperature (25–800 °C) and exposure time (30–3600 s) on the interaction between SO_2 gas and volcanic glasses of different composition (i.e., tephrite, phonolite, dacite and rhyolite). All experiments were carried out under a 40 standard $cm^3 min^{-1}$ gas stream of 1 mol% SO_2 and 70 mol% air (helium balance). This SO_2 concentration falls within the range of measured high temperature volcanic gas and estimated eruption plume gas compositions (see section: Composition). Uptake of SO_2 gas on the glass was assessed based on the amount of soluble sulfate released upon leaching of the post-experiment material with ultrapure water. As depicted in Figure 5a, the phonolite, dacite and rhyolite glasses displayed a consistent pattern of SO_2 uptake, corresponding to negligible sulfation below 400 °C followed by a sharp increase up to 700 °C (phonolite and rhyolite) and above (dacite). Sulfation of the tephrite glass surface began at a lower temperature (300 °C) but showed a similar trend. Crystalline $CaSO_4$ (anhydrite) was confirmed as the primary reaction product on the glass surfaces, with the fraction of Ca from the bulk glass incorporated into $CaSO_4$ deposits paralleling the amount of sulfation (Fig. 5b). Calcium sulfate is a compound stable up to approximately 1200 °C (Newman 1941). Remarkably, up to 50% of the bulk Ca content in the phonolite and rhyolite glasses was converted to $CaSO_4$ at 800 °C.

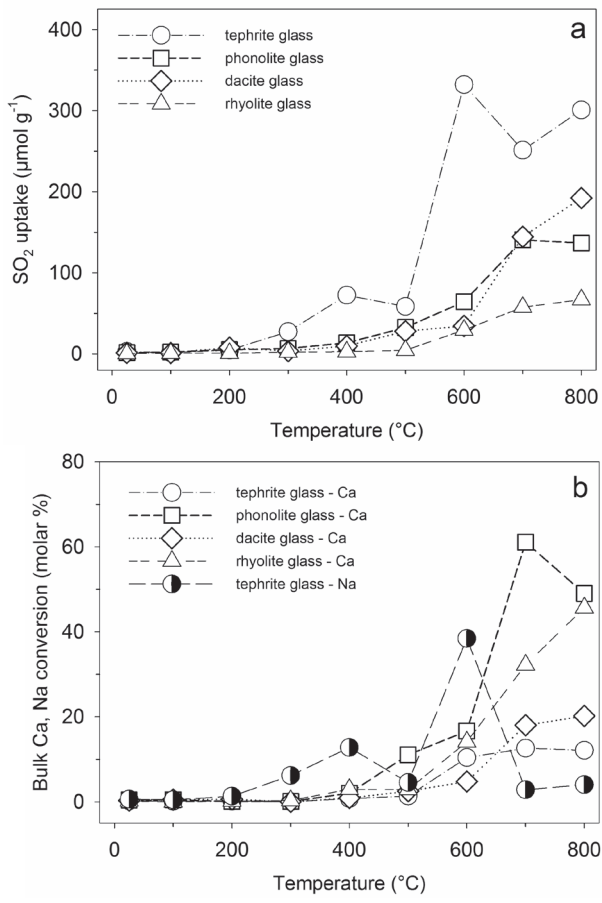


Figure 5. Amount of (a) SO_2 gas taken up by the volcanic glasses, and (b) mole percent of glass bulk Ca or Na converted to sulfate salts at the glass surface, upon exposure to SO_2 gas for 3600 s at various temperatures. The relative uncertainty on the uptake of SO_2 is ±15%. Modified after Ayris et al. (2013).

In order to maintain the extensive growth of $CaSO_4$ at the glass surface, Ayris et al. (2013) proposed that Ca migrates from the interior of the glass to its surface. Simple diffusion processes normally obey a relationship whereby the reaction quantity increases linearly with the square root of time. In a seminal paper, Douglas and Isard (1949) investigated the effect of anhydrous SO_2 gas on soda-lime–silica glass (Na_2O 16.8 wt%, CaO 5.4 wt%, SiO_2 69.9 wt%) at temperatures and exposures ranging, respectively, from 600 up to 800 °C and from minutes to days. Below 600 °C, the amount of sulfate formed on the glass surface was negligible, whereas at higher temperatures the kinetics were parabolic with time. While such relationships were not clearly evidenced in Ayris et al. (2013) for high temperature SO_2 uptake on the tephrite, phonolite, dacite and rhyolite glasses, TEM-EDX analyses revealed Ca-depleted regions located beneath the outer edges of the surface $CaSO_4$ deposits, extending several hundreds of nanometers into the bulk particle. Similarly, a subsequent independent study in which anorthosite was exposed to SO_2 at 800 °C for more than 41 h found strong Ca depletion in the vicinity of newly formed anhydrite crystals (Henley et al. 2015). Investigations of basalt and albite–anorthite–diopside glasses exposed to SO_2 at 700–800 °C for 1–24 h also showed $CaSO_4$ to be the dominant surface product, with Ca depletion in the sub-surface glass detected by nano-SIMS analysis (Palm et al. 2018, this volume; Renggli and King 2018, this volume) and laser ablation inductively coupled mass spectrometry (Palm et al. 2018, this volume). These experiments demonstrate that the reaction of SO_2 gas with Ca in the glass surface establishes a chemical potential gradient in the interior of the glass which drives the outward (from interior towards surface) diffusion of Ca.

In order to maintain the glass electroneutrality, the loss of Ca ions from the glass interior to the surface must be compensated. Previous dealkalization studies on soda-lime glasses which utilized SO_2 gas postulated co-diffusion of Ca^{2+} and O^{2-} (Douglas and Isard 1949; Mochel et al. 1966). In general, O^{2-} has a much lower diffusivity than the alkali and alkaline earth cations, although the difference attenuates with increasing temperature (Lamkin et al. 1992; Zhang et al. 2010). The activation energy of diffusion around the glass transition temperature is higher for O^{2-} ions than for the alkali and alkaline earth ions. Thus, it has been argued that the rate-limiting step of the dealkalization reaction in soda-lime glass is the motion of O^{2-} (Douglas and Isard 1949; Mochel et al. 1966).

In the case of a natural aluminosilicate glass (which contains multivalent cations such as $Fe^{2+/3+}$ and $Ti^{3+/4+}$) reacting with SO_2 at high temperatures, the diffusional transport of network modifier cations towards the surface may be compensated by the counter-diffusion of electron holes from one multivalent cation to another, rather than by an outward flux of O^{2-} (Renggli and King 2018, this volume). Such a mechanism reflects the higher diffusivity of electron holes compared to that of O^{2-}, which has been highlighted in oxidation experiments where surface reactions dominate; for example, when basaltic glass is subjected to atmospheric air around the glass transition temperature (Cooper et al. 1996; Cook and Cooper 2000; Burkhard 2001; Yue et al. 2009). Similarly, charge compensation through the motion of electron holes is likely to occur when an aluminosilicate glass is exposed to an oxidizing atmosphere such as a SO_2-rich gas mixture. Nevertheless, bulk O^{2-} diffusion may remain a plausible mechanism for charge-balancing an outward flux of alkali and alkaline earth cations (see section: Constraints on Ca and Na diffusion).

In aluminosilicate glasses, the mobile cations are the network modifiers, typically alkali and alkaline earth ions. Normally, the diffusion of alkali ions such as Na^+ and K^+ is faster due to their lower charge in comparison to alkaline earth ions (Varshneya 2006). In addition, the mobility of Mg^{2+} is expected to be greater than that of Ca^{2+} (Smedskjaer and Yue 2011; Renggli and King 2018, this volume). While Ayris et al. (2013) did not detect sodium sulfate (Na_2SO_4) or magnesium sulfate ($MgSO_4$) deposits on any of the SO_2-treated glasses, they measured significant Na extraction (up to ~40%) from the tephrite sample processed between 300 and 600 °C. Interestingly, this effect was not seen at higher temperatures (Fig. 5b), although Na_2SO_4 is stable up to and above 850 °C (Ebert et al. 1997). In contrast, Na_2SO_4 is

always the dominant salt that segregates on the surface of soda-lime–silica glass subjected to sulfur gas-supported dealkalization (e.g., Douglas and Isard 1949; Mochel et al. 1966). Other studies (Johnson and Burnett 1993; Li et al. 2010; Renggli and King 2018, this volume) also noticed the presence of multiple sulfates in experiments involving SO_2 gas and various silicate minerals and glasses (e.g., albite, diopside, soda-lime glass) and rock compositions (basalt, obsidian) at high temperatures (650–850 °C). Johnson and Burnett (1993) argued that alkali sulfate formation is favored when silicate glass displays low atomic Ca:Na ratio values (<0.25). However, this simple rule cannot explain the observations reported in Ayris et al. (2013), as the tephrite sample had the highest Ca:Na ratio (2.3) amongst all the glass compositions tested. Alternatively, these authors speculated that the absence of Na_2SO_4 formation in the SO_2-treated phonolite, dacite and rhyolite glasses could be a consequence of surface oxidation above their glass transition temperature. Specifically, oxidation of Fe^{2+} to Fe^{3+} (i.e., electron transfer) would lead to additional incorporation of Fe into tetrahedral coordination as a network former cation in the glass. This, in turn, could cause migration of Na^+ ion away from the surface to charge compensate Fe^{3+} in the glass network (Cook and Cooper 2000), thereby strongly reducing Na availability to form Na_2SO_4. This idea was proposed by Renggli and King (2018, this volume) who examined basaltic glasses with different Fe^{2+}:Fe^{3+} ratios. However, it remains unclear why this process apparently did not act in the tephrite glass to impede Na_2SO_4 formation. More research is needed to satisfactorily explain the complex factors that drive mobility of alkali and alkaline earth cations in multi-oxide silicate glass exposed to SO_2 gas at high temperatures.

While counter-diffusion of Ca^{2+} and electron holes (or possibly co-diffusion of Ca^{2+} and O^{2-}) in the glass probably drives $CaSO_4$ deposition on the surface, the mechanistic details of the high temperature heterogeneous reaction involving SO_2 gas and the volcanic glass surface components are not resolved. Sulfur dioxide is a dipolar molecule and in the gas phase it behaves as a Lewis acid. Thus, its chemisorption on aluminosilicate glass results preferentially from interaction with a basic surface oxide anion (i.e., O^{2-}), as presented by alkali alkaline earth oxides in the glass surface, effectively forming surface-bound sulfite (; e.g., Martin et al. 1987; Waqif et al. 1992; Schneider 2004). This is consistent with recent results showing that chemisorption of SO_2 gas on volcanic glass at room temperature ~~correlated~~ positively with its total surface Na, K, Mg and Ca content (Maters et al. 2017b). Similarly, sulfur retention on coal fly ash, a silica-dominated ~~multioxide~~ material containing glass, strongly and positively correlates with the weight percentage of alkali and alkaline earth metal oxides (e.g., Galloway et al. 2015, and references therein). Sulfur dioxide may also interact with Lewis acid surface sites, but such interaction is very weak as the bonding is largely electrostatic (Goodman et al. 2001) and accordingly, it most likely does not play a significant role under high temperature conditions.

Since $CaSO_4$ is the major surface product formed on volcanic glass exposed to SO_2 gas at temperatures up to 800 °C (e.g., Ayris et al. 2013), SO_2 molecules must first be adsorbed on the glass' Ca-O surface groups (≡Ca-O) which act as Lewis bases. Insights into the actual reaction mechanism may be gained from existing knowledge on the high temperature adsorption of SO_2 gas on porous solid calcium oxide (CaO). This reaction, which is utilized to remove sulfur from exhaust flue gases of fossil-fuel power plants, may serve as a conceptual analogue for the high temperature interaction of SO_2 gas with Ca-O groups present on the surface of aluminosilicate glass. Infrared spectroscopy and kinetic measurements show that at temperatures below 850 °C (i.e., those found within eruption plumes) and in the presence of gaseous oxygen (O_2), $CaSO_4$ formation is predominantly via a direct reaction between CaO and SO_2 gas. Experimental and modeling studies suggest that SO_2 forms a strongly bound chemisorbed complex on CaO that can best be described as a surface SO_3^{2-} anion (e.g., Martin et al. 1987; Karlsen et al. 2003; Schneider 2004). Subsequent oxidation of the so-formed calcium sulfite ($CaSO_3$) by O_2 produces $CaSO_4$. The sequence of reactions can be written as occurs as (Allen and Hayhurst 1996):

$$CaO_{(s)} + SO_{2(g)} \rightleftharpoons CaSO_{3(s)} \quad (1a)$$

$$CaSO_{3(s)} + 0.5O_{2(g)} \rightleftharpoons CaSO_{4(s)} \quad (1b)$$

The rate of sulfation by SO_2 is independent of O_2 concentration. At high temperature (>600 °C), $CaSO_3$ may start to decompose:

$$CaSO_{3(s)} \rightleftharpoons CaO_{(s)} + SO_{2(g)} \quad (2a)$$

However, this reaction does not inhibit sulfation as it is not favored in the presence of SO_2, even if the latter is at low pressure. In addition, sulfation of CaO is still possible via (Allen and Hayhurst 1996):

$$4CaO_{(s)} + 4SO_{2(g)} \rightleftharpoons 3CaSO_{4(s)} + CaS_{(s)} \quad (2b)$$

Calcium sulfite also has a thermodynamic tendency to disproportionate:

$$CaSO_{3(s)} \rightleftharpoons 0.75CaSO_{4(s)} + 0.25CaS_{(s)} \quad (3)$$

However, this reaction is slow (van Houte and Delmon 1978) and unlikely to be significant in eruption plumes. Finally, in the presence of O_2, any calcium sulfide (CaS) produced through reactions (2b) and (3) is oxidized:

$$CaS_{(s)} + 2O_{2(g)} \rightleftharpoons CaSO_{4(s)} \quad (4)$$

Reaction (4) can take place at temperatures above ~850 °C but is considerably slower than Reaction (1b) below ~850 °C.

For all glasses studied by Ayris et al. (2013), SO_2 gas uptake at 800 °C was rapid at the beginning of the experiment and slowed down thereafter (Fig. 6), although the time of transition between these two apparent regimes differed between samples. The average sulfation rates in the first 300–600 s were on the order of 0.1–0.4 µmol SO_2 g^{-1} ~~glass.s^{-1}~~ approximately

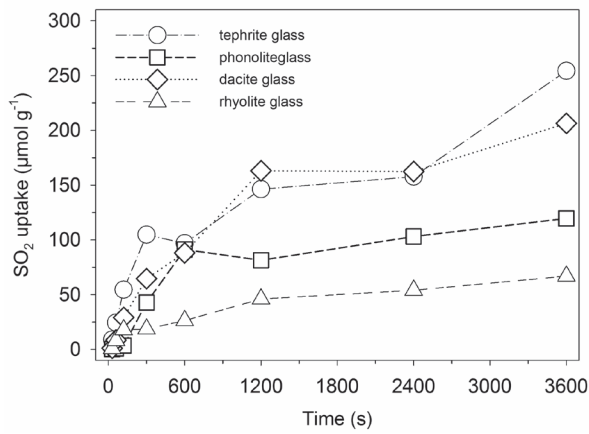


Figure 6. Amount of SO_2 gas taken up by the volcanic glasses upon exposure to SO_2 gas at 800 °C for various durations. The relative uncertainty on the uptake of SO_2 is ±15%. Modified after Ayris et al. (2013).

2.6– 9 times greater than the rates observed later. Allen and Hayhurst (1996) reported an initial sulfation rate of 4.4 µmol SO_2 $g^{-1}s^{-1}$ on solid CaO exposed to 0.6 vol% SO_2 in nitrogen at a temperature of ~830 °C. Accounting for the fact that the specific surface area of the volcanic glass material is roughly ten times lower than that of the CaO sample used in Allen and Hayhurst's study, the sulfation rates of the glass and CaO are surprisingly close. This may underpin the view that SO_2 uptake on volcanic glass below 850 °C proceeds via a reaction similar to that described for sulfation of CaO (Eqns. 1a and 1b). The decrease in SO_2 gas uptake rates observed at longer exposure times in Ayris et al.'s (2013) measurements may reflect occupation of most of the SO_2-reactive surface adsorption sites (surface passivation or poisoning) and appearance of a new factor controlling the uptake rate. This may include, for example, inter-particle resistance to SO_2 diffusion and/or decreasing access to Ca in the glass due to increasing surface coverage by $CaSO_4$ deposits (Kreider and Lipiński 2018, this volume; Renggli and King 2018, this volume; King et al. 2018, this volume).

Hydrogen chloride uptake and reaction

Hydrogen chloride is another important gas released from erupting magmas. A better understanding of its fate in eruption plumes has implications for correctly assessing the potential of stratospheric injection of volcanic gases that are involved in ozone destruction (Stolarski and Cicerone 1974). Previous works emphasized that in-plume HCl scavenging by hydrometeors (atmospheric particles of liquid or solid water formed by water condensation, deposition or freezing) is fast-acting and efficient, removing over 75% of erupted HCl within one hour of an eruption (Textor et al. 2003). On this basis, an influence of high temperature gas–ash interaction on the chemistry of HCl in eruption plumes has traditionally been discounted. However, combined with previous studies demonstrating that HCl gas reacts with soda-lime–silica glass compositions (e.g., Schaeffer et al. 1986; Sung et al. 2009), the ubiquitous presence of significant quantities of chloride salts on ash (e.g., Rose 1977; Durant et al. 2012) raises the possibility of substantial HCl uptake on ash at high temperatures in the eruption plume.

Ayris et al. (2014) tested this idea by probing the interaction between HCl gas and volcanic glass (the same four compositions as in their SO_2 study; Ayris et al. 2013) from 200 to 800 °C. Experiments were carried out by exposing the powdered material to 2 mol% HCl gas in helium for 3600 s. Across the four glass samples, only the tephrite and phonolite showed significant HCl uptake, with maximum and minimum uptake occurring in the temperature ranges of 400–600 °C and 700–800 °C, respectively (Fig. 7). Leachate, SEM, XPS and XRD

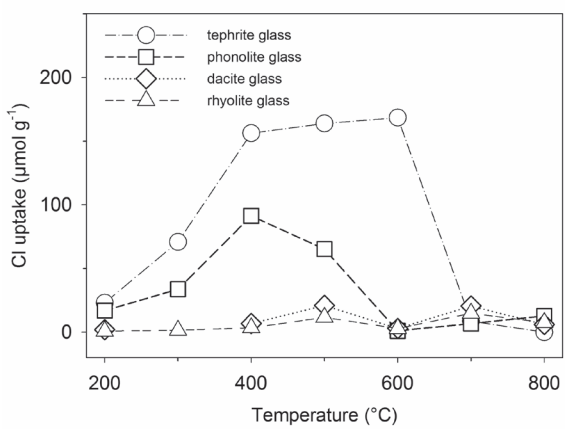


Figure 7. Amount of HCl gas taken up by the volcanic glasses upon exposure to HCl gas for 3600 s at various temperatures. The relative uncertainty on the uptake of HCl is ±15%. Modified after Ayris et al. (2014).

analyses of the post-experiment samples pointed to halite (NaCl) as the primary reaction product on both of these glasses up to 600 °C. Mobilization of other alkali and alkaline earth cations was negligible in these experiments.

By analogy with the binding of proton (H^+)-donating molecules to metal oxide surfaces (Henrich and Cox 1994), gaseous HCl molecules may first attach to Lewis acid metal cation sites on the aluminosilicate glass surfaces through their chloride (Cl^-) end. This is followed by spontaneous dissociation of the HCl bond with transfer of the H^+ to a surface Lewis base O^{2-} site. Since NaCl is the main reaction product formed upon exposure of volcanic glass to HCl glass at high temperatures, one may suspect that the adsorption sites are associated predominantly with ~~Na.~~ Nevertheless, other metal cations in the surface glass network, such as Al^{3+}, K^+, Ca^{2+}, and Mg^{2+} could also accommodate HCl adsorption. Again, new studies would help to unravel the reaction mechanisms leading to chemisorption of HCl gas on volcanic glass.

The findings of Ayris et al. (2014) agree well with those reported for dealkalization treatments of soda-lime–silica glass utilizing HCl gas at temperatures up to 700 °C (Boggs and Mosher 1956; Schaeffer et al. 1986). In this process, formation of NaCl on the glass surface is posited to proceed by diffusion of H^+ or H_3O^+ from the adsorbed HCl into the glass and of Na^+ ions from the glass bulk to the surface. This phenomenon is supported by Ayris et al. (2014)'s ~~STEM~~-EDX analyses of the tephrite glass surface exposed to HCl gas at 400 °C, which revealed Na-depleted regions located beneath the NaCl deposits and spanning more than one micrometer into the glass bulk. The contrasting reactivity towards HCl gas of the tephrite and phonolite versus the dacite and rhyolite was proposed to relate to effects of glass composition on the mobility of Na (e.g., mixed alkali effect; large variation in silicate glass physical properties relating to diffusivity—such as resistivity and viscocity—as one alkali ion is replaced by another; Mysen and Richet 2005). However, further investigations using for example tracer diffusion techniques or molecular dynamics simulations would be needed in order to shed light on such complex and largely unconstrained processes.

The near-complete cessation of HCl gas uptake on the tephrite glass above 600 °C noticed by Ayris et al. (2014) may relate to condensation of adjacent ≡Si–OH groups on the glass surface to ≡Si–O–Si≡ groups, thus forming a silica-like surface layer which impedes ion diffusion in and out of the glass (Schaeffer et al. 1986). As shown elsewhere for other glass types, the onset temperature at which glass network densification via surface dehydroxylation appears to affect the tephrite and phonolite samples in Ayris' experiments approximately coincides with their glass transition temperature (i.e., ~591 and ~637 °C, respectively).

Effect of mixed gas atmospheres

The effect of mixed gases on total gas uptake on aluminosilicate glasses at high temperatures has received little attention, yet the eruptive gas phase in a volcanic plume is a cocktail of different species spanning a large range of concentrations. Plume gases are typically dominated by water vapor and CO_2 gas and these compounds may interact with the erupted ash material. While none of the experiments by Ayris et al. (2013, 2014) reported above involved water vapor, previous dealkalization studies of commercial glass may offer some useful clues on the effect of a hydrous atmosphere on SO_2 and HCl gases uptake and reaction on volcanic glass.

Douglas and Isard (1949) observed that Na_2SO_4 formation on the surface of soda-lime–silica glass exposed to SO_2 gas proceeded significantly faster in the presence of water vapor, although this effect was notable only below 600 °C. This result could indicate that slow O^{2-} diffusion through the glass network is no longer needed in order to preserve glass electrical neutrality. For example, diffusion of H^+ derived from water vapor into the glass can rapidly compensate loss of Na^+ ion, to accomplish charge balance. Similarly, Sung et al. (2009) highlighted the role of water vapor in considerably enhancing the uptake of HCl gas (and the

outflux of Na) on a soda-lime-silica glass treated at 550 °C. The authors attributed such an effect to inhibition of glass dehydration at high water vapor concentration. In a dry atmosphere, Na^+ replacement by H^+ (or H_3O^+) is normally followed by dehydration and compaction of the silicate network according to (Sung et al. 2009):

$$2\,HCl_{(g)} + 2{\equiv}Si{-}ONa \rightleftharpoons 2\,NaCl_{(s)} + 2{\equiv}Si{-}OH \quad (5a)$$

and

$$2{\equiv}Si{-}OH \rightleftharpoons {\equiv}Si{-}O{-}Si{\equiv} + H_2O_{(g)} \quad (5b)$$

However, when water vapor is present, the dehydration will be inhibited and compaction will not take place:

$$H_2O_{(g)} + HCl_{(g)} + {\equiv}Si{-}ONa \rightleftharpoons NaCl_{(s)} + {\equiv}Si{-}OH + H_2O_{(g)} \quad (5c)$$

Taken together, these observations imply that uptake and reaction of SO_2 and HCl gases on glassy ash in an eruption plume may be favored by the presence of abundant water vapor, although its specific influence on alkali versus alkaline earth cation diffusion in glasses must still be assessed.

Ayris et al. (2013) showed that $CaSO_4$ is the dominant surface product in SO_2-volcanic glass reactions above 600 °C, while Ayris et al. (2014) demonstrated that in HCl-volcanic glass reactions NaCl is the major surface product. In these single-gas systems, other sulfate or chloride salts were only minor constituents of the final surface composition. Therefore, SO_2 and HCl gases in eruption plumes would not be expected to significantly compete for cations in an ash particle. Approximately 1:1 molar ratios of $Ca:SO_4$ and Na:Cl in ultrapure water leachates of natural ash may support the dominance of these cations and anions in the form of $CaSO_4$ and NaCl on ash surfaces (Rose et al. 1973; Rose 1977; Smith et al. 1983; de Hoog et al. 2001). Being a weaker Lewis acid (Waqif et al. 1992), CO_2 is also unlikely to alter SO_2 capture by ash, despite a greater concentration of the former gas in the eruptive gas phase. There is also no evidence in the scientific literature of calcium carbonate formation on ash. This leads us to speculate that mixed SO_2-HCl gases in the hot core of eruption plumes would be taken up at the rates predicted by single-gas experiments.

Finally, HF gas may be present in eruption plumes involving fluorine-rich magmas, although typically in lower abundance (<0.5 mol%) than SO_2 and HCl gases. It is well known that in the presence of water vapor, HF gas readily reacts with silica surfaces and that there is a dynamic balance between water, HF and hexafluorosilicic acid (H_2SiF_6) according to (e.g., Holmes and Snell 1966; van der Heide et al. 1989):

$$SiO_{2(s)} + 6\,HF_{(g)} \rightleftharpoons H_2SiF_{6(g/l)} + 2\,H_2O_{(g)} \quad (6a)$$

$$H_2SiF_{6(g/l)} \rightleftharpoons SiF_{4(g)} + 2\,HF_{(g)} \quad (6b)$$

Studies on $HF_{(g)}$-ash interactions are scarce in large part due to the danger of working with this gas. Óskarsson (1980) exposed pre-washed ash from Hekla volcano, Iceland, to a boiling HF-H_2O mixture at temperatures from 150 to 1100 °C. Analyses of the treated ash showed evidence of calcium hexafluorosilicate ($CaSiF_6$) and calcium fluoride (CaF_2) formed predominantly below and above ~600–700 °C, respectively. It was also proposed that sodium fluoride (NaF) is produced by HF-ash reaction. Future experimental work will have an important role to play in assessing potential competition between SO_2, HCl and HF in forming alkali- and alkaline earth-bearing reaction products on ash surfaces in eruption plumes.

MODELING THE UPTAKE OF SULFUR DIOXIDE AND HYDROGEN CHLORIDE GASES ON VOLCANIC ASH

Constraints on Ca and Na diffusion

As discussed above, there is strong compelling evidence that it is a diffusive transport process supplying mass to drive salt (i.e., mainly $CaSO_4$ and NaCl) growth on glass surfaces exposed to SO_2 or HCl gas. Ash from large explosive eruptions is often dominated by the glassy constituent, and if ash is approximated as spherical particles with a given radius R, then the kinetics of this process scale with the characteristic Fickian diffusion time $\lambda_d = R^2/D$, where D is the diffusion coefficient (or "diffusivity") of the species in question (e.g., Crank 1975). In volcanic ash, D is typically strongly dependent on temperature and weakly dependent on the absolute local amount of the diffusing species (Zhang and Ni 2010). Additionally, volcanic ash is typically polydisperse in size distribution such that bulk scaling of the diffusion kinetics would require R^3/R^2 ~~using~~ in place of R in computing λ_d (where R^n is the nth moment of the particle size distribution). Fick's diffusion in spherical coordinates is:

$$\frac{\partial C}{\partial t} = \frac{1}{r^2}\frac{\partial}{\partial r}\left(r^2 D \frac{\partial C}{\partial r}\right) \tag{7}$$

where C is the concentration of a given cation, t is the time, and r is the radial position in the ash particle from the center (Crank 1975). If D as a function of the local value of C is known, a full numerical solution to Equation (7) gives the spatial variation of $C(\cancel{T})$, which can be used to directly predict the amount of gas that is taken up by ash per unit time, assuming it is directly proportional to the amount of the relevant cations that can be supplied to the surface by diffusion (i.e., that the uptake is diffusion limited).

Ayris et al. (2013) used an analytical approximation of a full solution to Fick's diffusion equation (Eqn. 7) in which they made the simplifying assumption that D was only dependent on temperature (), in order to demonstrate that D for Ca supply to rhyolitic ash surfaces could be parameterized using isothermal experimental time-series data (60–3600 s exposures of rhyolitic glass particles to SO_2-helium atmospheres at 800 °C). They accounted for polydispersivity of the ash size distribution by using a weighted sum of the contribution of each size class of particle. In doing so, they recovered a D value broadly consistent with Mungall et al. (1999) who measured $D(T)$ directly by diffusion-couple experiments. In both cases, the form of $D(T)$ is Arrhenius and given by:

$$D(T) = D_\alpha \exp\left(-\frac{\alpha}{T}\right) \tag{8}$$

where D_α is a reference diffusivity and α is a reference temperature. As a quantitative example, Mungall et al. (1999) found that $D_\alpha = 2.54 \times 10^{-5}\ m^2 s^{-1}$ and $\alpha = 29830$ K for Ca diffusivity in a rhyolitic glass, and Zhang et al. (2010) found good agreement across a range of published data for Na diffusion in rhyolites using $D_\alpha = 1.34 \times 10^{-6}\ m^2 s^{-1}$ and $\alpha = 10210$ K. In both cases, the dependence of D on concentration is neglected. Given that the direct experimental evidence suggests that up to ~50% of the bulk Ca can be fed to ash particle surfaces by this diffusive process in the early high temperature region of large eruption plumes, the additional dependence of D on the local concentration of each cation may be important, and would require a different functional form in place of Equation (8).

These constraints are especially valid in the high temperature regime where D values are calibrated. Dingwell (1990) proposed that there is a high temperature regime in which the

diffusivity of the O^{2-} ions in the silicate structure, as approximated by the Eyring equation, can be used as a measure of bulk network mobility. The Eyring equation is expressed as ~~(e.g., Glasstone et al. 1941)~~:

$$D = kT / (l\mu) \quad (9)$$

where k is Boltzmann's constant, μ is the liquid viscosity, and l is the effective jump distance of oxygen atoms in the silicate structure (Glasstone et al. 1941; Dingwell 1990). Thus, in the high temperature regime (where viscosity is reduced), the diffusivity of cations such as Ca^{2+} and Na^{+} are coupled to the diffusivity of O^{2-} ions ~~on~~ the silicate structure. However, at lower temperatures, this relationship breaks and the diffusivity of the alkali and alkaline earth ions and that of O^{2-} ions are entirely decoupled (Dingwell 1990). These two regimes were referred to as intrinsic and extrinsic, respectively. The switch from the intrinsic to the extrinsic regime would therefore be predicted to occur during cooling in the plume, and would involve a shift in the activation energy for diffusive mass supply of cations to the ash surface.

This concept is illustrated in Figure 8, which shows the continuous curve for the Eyring diffusivity as calculated using Equation (9) and assuming $l \sim 0.5$ nm, consistent with the jump distance of oxygen in silicate melts (l has been found to be approximately constant across a large range of visocity and temperature) (Dingwell 1990). The normalization used in the Eyring equation implies that the diffusivity of a given species is limited by the mobility of the whole structural network, in this case represented by the viscosity. Early work suggested that the mobility of the network is in turn limited by the self-diffusivity of O^{2-} ions (e.g., Shimizu and Kushiro 1984). The results presented in Figure 8 effectively support the idea that oxygen reorganization, through glass network diffusion, is possible on the timescale of Ca mobility in the high temperature regime where melt viscosities are sufficiently low. This high temperature regime is only relevant in the proximal core of large eruption plumes.

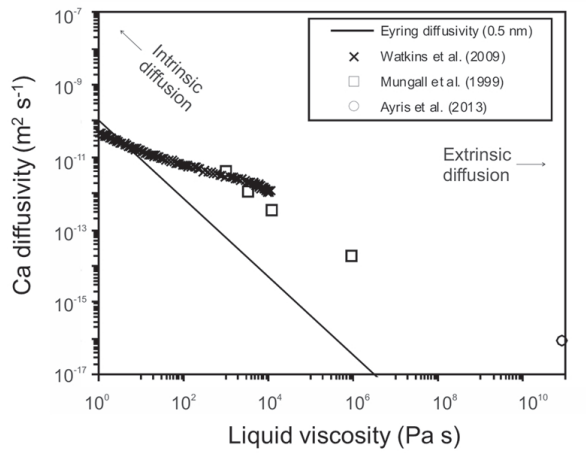


Figure 8. Diffusivity of Ca as a function of liquid viscosity using data from Mungall et al. (1999), Watkins et al. (2009) and Ayris et al. (2013). The solution of the Eyring diffusivity equation (see Eqn. 9 in the text) is calculated assuming a value of 0.5 nm for the jump distance l of oxygen in silicate melts (Dingwell~~,~~ 1990). ~~The shaded band represent the relative uncertainty on l~~. In the case of Mungall et al. (1999) and Watkins et al. (2009), the liquid viscosity was either directly measured or quoted in the work originitating in the data. Liquid viscosity for the Ayris et al. (2013) data point was calculated using the model of Hess and Dingwell (1996) and the 800 °C experimental temperature. The regimes of intrinsic diffusion (in the high temperature regime, low viscosity) and extrinsic diffusion (at lower temperature, higher viscosity) are labelled after Dingwell (1990).

The successful use of gas uptake experiments to invert for the value of D at a given temperature (e.g., Ayris et al. 2013, 2014) suggests that published $D(T)$ relationships, such as the examples given above, can be used to predict the timescales of diffusion in ash during dynamic cooling. Significantly, these findings also show that the rapid reactions at high temperature dominate, which in turn means that the total gas uptake can be predicted quantitatively.

Application to eruption plumes

As inferred from the work of Ayris et al. (2013, 2014), the total amount of SO_2 and HCl gases potentially removed by direct uptake on ash in explosive eruption plumes will depend on the ash composition and the duration over which the gas–ash mixture is sustained within the high temperature window (600–800 °C for SO_2, 400–600 °C for HCl) at which efficient adsorption occurs. Numerical models (e.g., Suzuki et al. 2005; Suzuki and Koyaguchi 2012) provide insight into the complex thermal regime of ash-laden eruption plumes as controlled by magma temperature and discharge rate, erupted magma volume, vent radius, and air entrainment by turbulent mixing. In the subterranean volcanic conduit, the gas–ash mixture produced by magma fragmentation may be sustained at temperatures >600 °C for seconds to minutes depending on the fragmentation depth and the post-fragmentation acceleration of the mixture (Ayris et al. 2013). Similar durations of exposure of the gas–ash mixture to high temperatures may occur in the subaerial volcanic plume (see section: *Temperature*), while the hot central core is insulated from the surrounding atmosphere (Ayris et al. 2014).

Adopting these time constraints, as well as the diffusion coefficient values (D for Ca and Na) at various temperatures determined for given glass compositions (i.e., tephrite, phonolite, dacite, rhyolite), the potential in-conduit/plume SO_2 and HCl uptake on glassy ash at high temperatures can be computed for different ash composition and gas:ash ratio scenarios. Taking the historical eruptions of Tambora in 1815 (30–45 km^3 erupted magma) and Krakatoa in 1883 (10–20 km^3 erupted magma) as examples, Ayris et al. (2013) concluded that SO_2 gas uptake on ash during ascent through a conduit of 1000–2000 and 4000–5000 m may scavenge up to 7 and 45% of the total SO_2 emitted, respectively. Using a similar approach and accounting for the potential influence of a hydrous atmosphere on HCl gas uptake, Ayris et al. (2014) predicted that HCl removal by ash is probably negligible in small explosive eruptions, but is likely to be orders of magnitude greater in large explosive eruptions. For example, for a large eruption comparable to that of Tambora in 1815, phonolitic ash could scavenge 100% (94 Tg) of the total HCl emitted.

While additional work is needed to assess the impact of the presence of other volatiles in the eruptive gas phase (see section: *Effect of Mixed Gas Atmospheres*) and of ash crystallinity on the SO_2 and HCl uptake efficiency, these model assessments of the extent of SO_2 and HCl gas reactions with ash across various eruption scenarios serve to illustrate that high temperature gas–ash interactions can potentially induce a significant reduction in the amount of volcanic sulfur and chlorine ultimately injected into the stratosphere.

SUMMARY AND CONCLUSIONS

An explosive volcanic eruption plume, being comprised of gases, ash particles and liquid aerosols under dynamic physical, chemical and thermal conditions, provides ample opportunities for a variety of heterogeneous reactions. In particular, reactions between the gas and ash components within the short-lived hot core of the eruption plume are of interest as these may partly dictate the fate of environmentally relevant magmatic volatiles such as sulfur and chlorine, as well as impart a distinct surface reactivity to the ash material that will subsequently be transported in the atmosphere and ultimately deposited to terrestrial or aquatic environments. For instance, the scavenging of SO_2 and HCl gases by ash surfaces may have important atmospheric and climate implications, reducing the availability of these gases for

secondary processes such as the formation of sulfate aerosols and the catalytic destruction of ozone (Stolarski and Cicerone 1974; Robock 2000; Cadoux et al. 2015). Moreover, upon deposition to land or water, the products of high temperature gas–ash reactions can have beneficial or detrimental impacts on living and non-living systems. Sulfate and halide salts may be readily mobilized from ash surfaces into the surroundings, for example bringing a fresh supply of nutrients to soils and plants or potentially contaminating soil and water resources, with risk to animals and humans (Ayris and Delmelle 2012, and references therein).

The hot core of an eruption plume is inaccessible to direct study but new laboratory experiments, in which a range of chemical and thermal conditions relevant to eruption plumes can be simulated, are improving our understanding of high temperature gas–ash interactions (Ayris et al. 2013, 2014; Renggli and King 2018, this volume). Notably, these investigations show that SO_2 gas reacts with powdered aluminosilicate glasses (used as proxies for volcanic ash) most efficiently at temperatures of 600–800 °C to form $CaSO_4$ deposits. Sodium sulfate may also form but in minor amounts and below 600 °C. In the case of HCl gas, significant uptake on the glass material occurs at lower temperatures of 400–600 °C and results in the formation of NaCl deposits. In contrast to SO_2, negligible HCl uptake on silica-rich glass compositions highlights a strong compositional dependence.

The precise high temperature reaction mechanism leading to irreversible SO_2 gas uptake on aluminosilicate glass surfaces is not yet fully elucidated, but chemisorption of SO_2 probably occurs at basic surface sites presented by alkali and alkaline earth oxide groups. On the other hand, counter-diffusion of Ca and electron holes within the glass probably drives the growth of $CaSO_4$ crystals, sometimes accompanied by Na_2SO_4 formation, although the possibility of outward migration of O^{2-} as an alternative charge-balancing mechanism cannot be dismissed. By the same tenet, ~~interdiffusion~~, of H^+ from HCl gas into the glass and Na^+ from the glass bulk to its surface controls NaCl deposition in the HCl experiments, although further investigations are needed to understand the contrasting reactivities of different glass compositions, and relatedly, to unravel the reaction pathways leading to HCl gas chemisorption on aluminosilicate glass surfaces.

Using experimental data on SO_2 and HCl gas uptake on volcanic glasses, the values of D for Ca and Na at a given temperature can be computed. Combining these values (and more generally, published $D(T)$ relationships) with numerical models simulating the thermal regimes experienced by a gas–ash mixture under various eruption scenarios; one can quantitatively predict the timescales of diffusion in glassy ash during dynamic cooling and, thereby, the total gas uptake resulting from high temperature heterogeneous reactions in the plume. Such an approach suggests that negligible amounts to up to half of the SO_2 or all of the HCl gas emitted may be removed by glassy ash in the hot plume core. These findings emphasize that gas–ash reactions at high temperatures is an important mechanism for volcanic gas scavenging. Relatedly, they suggest an additional origin of the poorly described salt deposits on ash surfaces, apart from the traditional view that such salts precipitate at low ~~temperature~~, following dissolution of ash surface constituents by a low-pH aqueous film.

Assessment of the importance of high temperature gas–ash interactions to volcanic sulfur and halogen budgets will only improve with additional experimental and modeling studies. New studies will shed light on the mechanisms, and the conditions under which they operate, effecting charge balance for an outward diffusive flux of cations in an aluminosilicate glass exposed to SO_2. Moreover, there is a need for unravelling the influence of other potentially reactive gas species commonly found in volcanic eruption plumes, such as H_2O, H_2S and HF, on the reactions between ash particles and SO_2 and HCl gases and on the formation of secondary compounds on ash surfaces. Future research has an important role to play in further elucidating the underlying controls on and mechanisms of gas–ash reactions, and in better representing such reactions among the complexities of particle, gas and temperature dynamics within explosive eruption plumes.

ACKNOWLEDGEMENTS

Delmelle gratefully acknowledges support from a Vice-Chancellor University Anniversary Lectureship (University of York) and a FNRS grant (MIS-Ulysse F.6001.11). Maters benefited from a FNRS PhD studentship (Mandat Aspirant FC.88010). Ayris was funded by a NERC Blue Skies PhD studentship and an AXA Research Grant. We appreciate technical assistance from R. Sutton and D. Hay (Environment Department, University of York) and C. Givron and A. Iserentant (Environmental Sciences, Earth and Life Institute, Université catholique de Louvain). We thank C. Renggli, S. Gislason, R. Henley and P. King for helpful and constructive comments, and J. Vasseur and M. Rossi for thought-provoking discussions.

REFERENCES

Allen D, Hayhurst AN (1996) Reaction between gaseous sulfur dioxide and solid calcium oxide mechanism and kinetics. J Chem Soc Faraday Trans 92:1227–1238

Atkins PW, Jones LL (1999) Chemical Principles: The Quest for Insight. W. H. Freeman and Company, New York

Auroux A, Gervasini A (1990) Microcalorimetric study of the acidity and basicity of metal oxide surfaces. J Phys Chem 94:63–71

Ayris PM, Delmelle P (2012) The immediate environmental effects of tephra emission. B Volcanol 74:1905–1936

Ayris PM, Lee AF, Wilson K, Kueppers U, Dingwell DB, Delmelle P (2013) SO_2 sequestration in large volcanic eruptions: high-temperature scavenging by tephra. Geochim Cosmochim Acta 110:58–69

Ayris PM, Delmelle P, Cimarelli C, Maters EC, Suzuki YJ, Dingwell DB (2014) HCl uptake by volcanic ash in the high temperature eruption plume: Mechanistic insights. Geochim Cosmochim Acta 144:188–201

Ayris PM, Cimarelli C, Delmelle P, Wadsworth FB, Vasseur J, Suzuki YJ, Dingwell DB (2015) A novel apparatus for the simulation of eruptive gas-rock interactions. B Volcanol 77:104

Bagdassarov N, Dingwell D (1994) Thermal properties of vesicular rhyolite. J Volcanol Geoth Res 60:179–191

Boggs JE, Mosher HP (1956) Kinetics of the reaction of hydrogen chloride with glass. J Am Chem Soc 78:3901–3903

Brantley SL (2003) Reaction Kinetics of Primary Rock-forming Minerals under Ambient Conditions. *In:* Treatise on Geochemistry. Vol 5. Drever JI (ed) Elsevier, Amsterdam, p 73–117

Burkhard DJM (2001) Crystallization and oxidation of Kilauea basalt glass: processes during reheating experiments. J Petrol 42:507–27

Burgisser A, Degruyter W (2015) Magma Ascent and Degassing at Shallow Levels. *In:* The Encyclopedia of Volcanoes. Second Edition. Sigurdsson H, Houghton B, McNutt SR, Rymer H, Stix J (eds) Academic Press, London, p 225–236

Cadoux A, Scaillet B, Bekki S, Oppenheimer C, Druitt TH (2015) Stratospheric ozone destruction by the Bronze-Age Minoan eruption (Santorini Volcano, Greece). Sci Rep 5:12243

Carey S, Bursik M (2015) Volcanic Plumes. *In:* The Encyclopedia of Volcanoes. Second Edition. Sigurdsson H, Houghton B, McNutt SR, Rymer H, Stix J (eds) Academic Press, London, p 571–585

Carre A, Roger F, Varinot C (1992) Study of acid/base properties of oxide, oxide glass, and glass-ceramic surfaces. J Colloid Interf Sci 154:174–183

Cashman KV, Scheu B (2015) Magma Fragmentation. *In:* The Encyclopedia of Volcanoes. Second Edition. Sigurdsson H, Houghton B, McNutt SR, Rymer H, Stix J (eds) Academic Press, London, p 459–471

Cook GB, Cooper RF (2000) Iron concentration and the physical processes of dynamic oxidation in an alkaline earth aluminosilicate glass. Am Mineral 85:397–406

Cooper RF, Fanselow JB, Poker DB (1996) The mechanism of oxidation of a basaltic glass: Chemical diffusion of network-modifying cations. Geochim Cosmochim Acta 60:3253–3265

Crank J (1975) The Mathematics of Diffusion. Second Edition. Oxford University Press, Oxford

Cronin SJ, Neall VE, Lecointre JA, Hedley MJ, Loganathan P (2003) Environmental hazards of fluoride in volcanic ash: a case study from Ruapehu volcano, New Zealand. J Volcanol Geoth Res 121:271–291

Dahlgren RA, Saigusa M, Ugolini FC (2004) The nature, properties and management of volcanic soils. Adv Agron 82:113–182

Dalby KM, Mernagh TP, King PL, Hervig RL, Berger JA, Brand HEA, Eder K, Eggins SM, Herring A, Kreider PB, Palm AB, Renggli CJ, Troitzsch U, Cairney, JM (2018) Analytical techniques for probing small-scale layers that preserve information on gas-solid interactions. Rev Mineral Geochem 84:xxx-xxx

Dawson J, Delbos E, Hough R, Lumsdon D, Mayes B, Watson H (2011) Impacts of volcanic ash originating from the April 2010 eruption in Eyjafjallajökull (Iceland) on the natural resources of Scotland. The Macaulay Land Use Research Institute, Aberdeen

de Hoog JCM, Koetsier GW, Bronto S, Sriwana T, van Bergen MJ (2001) Sulfur and chlorine degassing from primitive arc magmas: temporal changes during the 1982–1983 eruptions of Galunggung (West Java, Indonesia). J Volcanol Geoth Res 108:55–83

Delmelle P, Villiéras F, Pelletier M (2005) Surface area, porosity and water adsorption properties of fine volcanic ash particles. B Volcanol 67:160–169
Delmelle P, Lambert M, Dufrêne Y, Gerin P, Óskarsson N (2007) Gas/aerosol–ash interaction in volcanic plumes: new insights from surface analyses of fine ash particles. Earth Planet Sci Lett 259:159–170
de Moor JM, Fischer TP, Hilton DR, Hauri E, Jaffe LA, Camacho JT (2005) Degassing at Anatahan volcano during the May 2003 eruption: Implications from petrology, ash leachates, and SO_2 emissions. J Volcanol Geoth Res 146:117–138
Dingwell DB (1990) Effects of structural relaxation on cationic tracer diffusion in silicate melts. Chem Geol 82:209–216
Douglas RW, Isard JO (1949) The action of water and of sulphur dioxide on glass surfaces. J Soc Glass Tech 33:289–335
Duggen S, Olgun N, Croot P, Hoffmann L, Dietze H, Delmelle P, Teschner C (2010) The role of airborne volcanic ash for the surface ocean biogeochemical iron-cycle: a review. Biogeosciences 7:827–844
Durant AJ, Villarosa G, Rose WI, Delmelle P, Prata AJ, Viramonte JG (2012) Long-range volcanic ash transport and fallout during the 2008 eruption of Chaitén volcano, Chile. Phys Chem Earth A/B/C 45:50–64
Ebert WL, Rosine SD, Bakel AJ (1997) Gas Evolution During Vitrification of Sodium Sulfate and Silica. Argonne National Laboratory, United States Department of Energy, Office of Environmental Restoration and Waste Management, Argonne
Fischer TP, Chiodini G (2015) Volcanic, Magmatic and Hydrothermal Gases. *In:* The Encyclopedia of Volcanoes. Second Edition. Sigurdsson H, Houghton B, McNutt SR, Rymer H, Stix J (eds) Academic Press, London, p 779–797
Fisher RV, Schmincke HU (1984) Pyroclastic Rocks. Springer-Verlag, Berlin
Fowler AC, Scheu B (2016) A theoretical explanation of grain size distributions in explosive rock fragmentation. Proc Roy Soc A 472:20150842
Fripiat JJ, Léonard A, Uytterhoeven JB (1965) Structure and properties of amorphous silicoaluminas. II. Lewis and Brønsted acid sites. J Phys Chem 69:3274–3279
Galloway BD, Sasmaz E, Padak B (2015) Binding of SO_3 to fly ash components: CaO, MgO, Na_2O and K_2O. Fuel 145:79–83
Gerlach TM (2004) Volcanic sources of tropospheric ozone-depleting trace gases. Geochem Geophys Geosy 5:Q09007
Gislason SR, Hassenkam T, Nedel S, Bovet N, Eiriksdottir ES, Alfredsson HA, Hem CP, Balogh ZI, Dideriksen K, Óskarsson N, Sigfusson B, Larsen G, Stipp SLS (2011) Characterization of Eyjafjallajökull volcanic ash particles and a protocol for rapid risk assessment. P Natl Acad Sci 108:7307–7312
Glasstone S, Laidler KJ, Eyring H (1941) The Theory of Rate Processes. McGraw-Hill, New York
Goodman AL, Li P, Usher CR, Grassian VH (2001) Heterogeneous uptake of sulfur dioxide on aluminum and magnesium oxide particles. J Phys Chem A 105:6109–6120
Gottsmann J, Giordano D, Dingwell DB (2002) Predicting shear viscosity during volcanic processes at the glass transition: A calorimetric calibration. Earth Planet Sci Lett 198:417–427
Grainger RG, Highwood EJ (2003). Changes in stratospheric composition, chemistry, radiation and climate caused by volcanic eruptions. *In:* Volcanic Degassing. Oppenheimer C, Pyle DM, Barclay J (eds) Geological Society Special Publications, London, 213, p 329–347
Hamme RC, Webley PW, Crawford WR, Whitney FA, DeGrandpre MD, Emerson SR, Eriksen CC, Giesbrecht KE, Gower JFR, Kavanaugh MT, Peña MA, Sabine CL, Batten SD, Coogan LA, Grundle DS, Lockwood D (2010) Volcanic ash fuels anomalous plankton bloom in subarctic northeast Pacific. Geophys Res Lett 37:L19604
Heiken G, Wohletz K (1992) Volcanic Ash. University of California Press, London
Helgeson HC, Murphy WM, Aagaard P (1984) Thermodynamic and kinetic constraints on reaction rates among minerals and aqueous solutions. II. Rate constants, effective surface area, and the hydrolysis of feldspar. Geochim Cosmochim Acta 48:2405–2432
Henley RW, King PL, Wykes JL, Renggli CJ, Brink FJ, Clark DA, Troitzsch U (2015) Porphyry copper deposit formation by sub-volcanic sulphur dioxide flux and chemisorption. Nat Geosci 8:210–215
Henrich VE, Cox PA (1994) The Surface Science of Metal Oxides. Cambridge University Press, Cambridge
Hess KU, Dingwell DB (1996) Viscosities of hydrous leucogranitic melts: A non-Arrhenian model. Am Mineral 81:1297–1300
Hinkley TK, Smith KS (1982) Leachate chemistry of ash from the May 18, 1980 eruption of Mount. St. Helens. U.S. Geol Surv Prof Pap 1397-B:27–64
Holloway JR, Wood BJ (1988) Simulating the Earth: Experimental Geochemistry. Unwin Hyman, Boston
Holmes PJ, Snell JE (1966) A vapour etching technique for the photolithography of silicon dioxide. Microelectronics and Reliab 5:337–341
Hoshyaripour G, Hort M, Langmann B (2012) How does the hot core of a volcanic plume control the sulfur speciation in volcanic emission? Geochem Geophys Geosy 13:Q07004
Hoshyaripour GA, Hort M, Langmann B (2015) Ash iron mobilization through physicochemical processing in volcanic eruption plumes: a numerical modeling approach. Atmos Chem Phys 15:9361–9379

Johnson ML, Burnett DS (1993) SO_2–rock interaction on Io: Reaction under highly oxidizing conditions. J Geophys Res-Planet 98:1223–1230

Jones TJ, McNamara K, Eychenne J, Rust AC, Cashman KV, Scheu B, Edwards R (2016) Primary and secondary fragmentation of crystal-bearing intermediate magma. J Volcanol Geoth Res 327:70–83

Kameda M, Ichihara M, Shimanuki S, Okabe W, Shida T (2013) Delayed brittle-like fragmentation of vesicular magma analogue by decompression. J Volcanol Geoth Res 258:113–125

Karlsen EJ, Nygren MA, Pettersson LGM (2003) Comparative study on structures and energetics of NOx, SOx, and COx adsorption on alkaline-earth-metal oxides, J Chem Phys B 107:7795–7802

King PL, Renggli C, Wheeler V, Palm A, Guan Y, Vennemann T, Kreider P, Troitzsch Y, Wilson S, Harrison A, Morgan B, Yue L, Mernagh TP, Nekvasil H, Leshin LA, Branson O, Brand HEA, Lipiński W, Baile R (2018) Experimental approaches and theoretical aspects of gas–solid reactions. Rev Mineral Geochem 84:xxx-xxx

Kreider P, Lipiński W (2018) High-temperature gas-solid heterogenous reactions in industrial processes. Rev Mineral Geochem 84:xxx-xxx

Kueppers U, Scheu B, Spieler O, Dingwell DB (2006) Fragmentation efficiency of explosive volcanic eruptions: A study of experimentally generated pyroclasts. J Volcanol Geoth Res 153:125–135

Lamkin MA, Riley FL, Fordham RJ (1992) Oxygen mobility in silicon dioxide and silicate glasses: a review. J Eur Ceram Soc 10:347–367

Legrand AP (1998) The Surface Properties of Silicas. John Wiley & Sons, Chichester

Li EY, Chareev A, Shilobreeva SN, Grichuk DV, Tyutyunnik OA (2010) Experimental study of sulfur dioxide interaction with silicates and aluminosilicates at temperatures of 650 and 850 °C. Geochem Int 48:1039–1046

Mader HM, Llewellin EW, Mueller SP (2013) The rheology of two-phase magmas: a review and analysis. J Volcanol Geoth Res 257:135–158

Martin MA, Childers JW, Palmer RA (1987) Fourier transform infrared photoacoustic spectroscopy characterization of sulfur-oxygen species resulting from the reaction of SO_2 with CaO and $CaCO_3$. Appl Spectrosc 41:120–126

Maters EC, Delmelle P, Rossi MJ, Ayris PM, Bernard A (2016) Controls on volcanic ash surface reactivity investigated with probe gases. Earth Planet Sci Lett 450:254–262

Maters EC, Delmelle P, Gunnlaugsson HP (2017a) Controls on iron mobilisation from volcanic ash at low pH: Insights from dissolution experiments and Mössbauer spectroscopy. Chem Geol 449:73–81

Maters EC, Delmelle P, Rossi MJ, Ayris PM (2017b) Reactive uptake of sulfur dioxide and ozone on volcanic glass and ash at ambient temperature. J Geophys Res-Atmos 122:10077–10088

McDonald RS (1958) Surface functionality of amorphous silica by infrared spectroscopy. J Phys Chem 62:1168–1178

Mernagh TP, King PL, McMillan PF, Berger JA and Dalby KN (2018) Using infrared and Raman spectroscopy to analyze gas-solid reactions. Rev Mineral Geochem 84:xxx-xxx

Mochel EL, Nordberg ME, Elmer TH (1966) Strengthening of glass surfaces by sulfur trioxide treatment. J Am Ceram Soc 49:585–589

Mueller SB, Ayris PM, Wadsworth FB, Kueppers U, Casa AS, Delmelle P, Taddeucci J, Jacob M, Dingwell DB (2017) Ash aggregation enhanced by deposition and redistribution of salt on the surface of volcanic ash in eruption plumes. Nature Sci Rep 7:45762

Mungall JE, Dingwell DB, Chaussidon M (1999) Chemical diffusivities of 18 trace elements in granitoid melts. Geochim Cosmochim Acta 63:2599–2610

Mysen B, Richet P (2005) Silicate Glasses and Melts. Vol 10. Elsevier B.V., Amsterdam

Newman ES (1941) Behavior of calcium sulfate at high temperatures. J Re Natl Bur Stand 17:191–196

Óskarsson N (1980) The interaction between volcanic gases and tephra: fluorine adhering to tephra of the 1970 Hekla eruption. J Volcanol Geoth Res 8:251–266

Palm AB, King PL, Renggli CJ, Hervig RL, Dalby KN, Herring A, Mernagh TP, Eggins SM, Troitzsch U, Beeching L, Kinsley L, Guagliardo P (2018) Unravelling the consequences of SO_2—basalt reactions for geochemical fractionation and mineral formation. Rev Mineral Geochem 84:xxx-xxx

Paukshtis EA, Kotsarenko NS, Karakchiev LG (1979) Investigation of proton-acceptor properties of oxide surfaces by IR spectroscopy of hydrogen-bonded complexes. React Kinet Catal Lett 12:315–319

Renggli CJ, King PL (2018) Changes in mineralogy and chemistry resulting from SO_2 gas reactions with silicate glasses. Rev Mineral Geochem 84:xxx-xxx

Riley CM, Rose WI, Bluth GJS (2003) Quantitative shape measurements of distal volcanic ash. J Geophys Res-Sol Ea 108:2504

Robock A (2000) Volcanic eruptions and climate. Rev Geophys 38:191–219

Rose WI (1977) Scavenging of volcanic aerosol by ash: atmospheric and volcanological implications. Geology 5:621–624

Rose WI, Bonis S, Stoiber RE, Keller M, Bickford T (1973) Studies of volcanic ash from two recent Central American eruptions. B Volcanol 37:338–364

Schaeffer HA, Stengel M, Mecha J (1986) Dealkalization of glass surfaces utilizing HCl gas. J Non-Cryst Solids 80:400–404

Schneider WF (2004) Qualitative differences in the adsorption chemistry of acidic (CO_2, SO_x) and amphiphilic (NO_x) species on the alkaline earth oxides. J Phys Chem B 108:273–282

Scholze H (1990) Glass. Nature, Structure, and Properties. Springer-Verlag, London
Shimizu N, Kushiro I (1984) Diffusivity of oxygen in jadeite and diopside melts at high pressures. Geochim Cosmochim Acta 48:1295–1303
Smedskjaer MM, Yue Y (2011) Inward and outward diffusion of modifying ions and its impact on the properties of glasses and glass-ceramics. Int J App Glass Sci 2:117–128
Smith DB, Zielinski RA, Taylor HE, Sawyer MB (1983) Leaching characteristics of ash from the May 18, 1980, eruption of Mount St. Helens volcano, Washington. B Volcanol 46:103–123
Sparks RSJ, Bursik MI, Carey SN, Gilbert JS, Glaze LS, Sigurdsson S, Woods AW (1997) Volcanic Plumes. John Wiley & Sons, London
Stolarski RS, Cicerone RJ (1974) Stratospheric chlorine: a possible sink for ozone. Can J Chem 52:1610–1615
Sung HJ, Noda R, Horio M (2009) Coupled recycling of PVC and glass wastes producing chlorine-free fuels and cement feed stock. Environ Sci Technol 43:47–52
Suzuki YJ, Koyaguchi T (2012) 3-D numerical simulations of eruption column collapse: effects of vent size on pressure balanced jet/plumes. J Volcanol Geoth Res 221:1–13
Suzuki YJ, Koyaguchi T, Ogawa M, Hachisu I (2005) A numerical study of turbulent mixing in eruption clouds using a three-dimensional fluid dynamics model. J Geophys Res 110:B08201
Tanabe K, Misono M, Ono Y, Hattori H (1989) New Solid Acids and Bases: Their Catalytic Properties. Elsevier Science Publishers, Amsterdam
Taylor PS, Stoiber RE (1973) Soluble material on ash from active Central American volcanoes. Geol Soc Am Bull 84:1031–1042
Textor C, Graf H-F, Herzog M, Oberhuber JM (2003) Injection of gases into the stratosphere by explosive volcanic eruptions. J Geophys Res 108:4606
Thorarinsson S (1979) On the damage caused by volcanic eruptions with special reference to tephra and gases. *In:* Volcanic Activity and Human Ecology. Sheets PD, Grayson DK (eds) Academic Press, New York, p 125–159
Tie XX, Brasseur G (1995) The response of stratospheric ozone to volcanic eruptions: Sensitivity to atmospheric chlorine loading. Geophys Res Lett 22:3035–3038
van der Heide PAM, Baan Hofman MJ, Ronde HJ (1989) Etching of thin SiO_2 layers using wet HF gas. J Vac Sci Tecnol 3:1719–1723
van Houte G, Delmon B (1978) Kinetics of the reaction of calcium sulfite with SO_2. Bull Soc Chim Belges 87:241–249
Varekamp JC, Luhr JF, Prestegaard KL (1984) The 1982 eruptions of El Chichón Volcano (Chiapas, Mexico): character of the eruptions, ash-fall deposits, and gasphase. J Volcanol Geoth Res 23:39–68
Varshneya AK (2006) Fundamentals of Inorganic Glasses. Society of Glass Technology, Sheffield
von Glasow R, Bobrowski N, Kern C (2009) The effects of volcanic eruptions on atmospheric chemistry. Chem Geol 263:131–142
Wadsworth FB, Vasseur J, Llewellin EW, Genareau K, Cimarelli C, Dingwell DB (2017) Size limits for rounding of volcanic ash particles heated by lightning. J Geophys Res-Sol Ea 122:1977–1989
Waqif M, Saad AM, Bensitel M, Bachelier J, Saur O, Lavalley J-C (1992) Comparative study of SO_2 adsorption on metal oxides. J Chem Soc Faraday Trans 88:2931–2936
Watkins JM, DePaolo DJ, Huber C, Ryerson FJ (2009) Liquid composition-dependence of calcium isotope fractionation during diffusion in molten silicates. Geochim Cosmochim Acta 73:7341–7359
Witham CS, Oppenheimer C, Horwell CJ (2005) Volcanic ash-leachates: a review and recommendations for sampling methods. J Volcanol Geoth Res 141:299–326
Yue YZ, Korsgaard M, Kirkegaard LF, Heide G (2009) Formation of a nanocrystalline layer on the surface of stone wool fibers. J Am Ceram Soc 92:62–67
Zhang Y, Ni H (2010) Diffusion of H, C, and O components in silicate melts. Rev Mineral Geochem 72:171–225
Zhang Y, Ni H, Chen Y (2010) Diffusion data in silicate melts. Rev Mineral Geochem 72:311–408